Development 134, 2027-2039 (2007) doi:10.1242/dev.02849

Enabled plays key roles in embryonic epithelial morphogenesis in *Drosophila*

Julie Gates[1,2], James P. Mahaffey[1], Stephen L. Rogers[1], Mark Emerson[3], Edward M. Rogers[1], Stephanie L. Sottile[2], David Van Vactor[3], Frank B. Gertler[4] and Mark Peifer[1,*]

Studies in cultured cells and in vitro have identified many actin regulators and begun to define their mechanisms of action. Among these are Enabled (Ena)/VASP proteins, anti-Capping proteins that influence fibroblast migration, growth cone motility, and keratinocyte cell adhesion in vitro. However, partially redundant family members in mammals and maternal Ena contribution in *Drosophila* previously prevented assessment of the roles of Ena/VASP proteins in embryonic morphogenesis in flies or mammals. We used several approaches to remove maternal and zygotic Ena function, allowing us to address this question. We found that inactivating Ena does not disrupt cell adhesion or epithelial organization, suggesting its role in these processes is cell type-specific. However, Ena plays an important role in many morphogenetic events, including germband retraction, segmental groove retraction and head involution, whereas it is dispensable for other morphogenetic movements. We focused on dorsal closure, analyzing mechanisms by which Ena acts. Ena modulates filopodial number and length, thus influencing the speed of epithelial zippering and the ability of cells to match with correct neighbors. We also explored filopodial regulation in cultured *Drosophila* cells and embryos. These data provide new insights into developmental and mechanistic roles of this important actin regulator.

KEY WORDS: Ena/VASP, Epithelial morphogenesis, Cytoplasmic transport, Adhesion, *Drosophila melanogaster*

INTRODUCTION

Embryonic development is remarkable – individual cells, by coordinated action, shape the body plan during morphogenesis. One challenge is to identify the molecular machinery involved and how it is used in different ways to perform a remarkably diverse set of behaviors. The actin cytoskeleton provides force for cell movement and shape change (Pollard and Borisy, 2003). Roles of many actin regulators were defined through studies in vitro, or in relatively simple systems such as budding yeast or fibroblasts. Even single cells deploy different actin modulators in different contexts, to construct actin structures required for each event: for example, one subset mediating cytokinesis while an overlapping but non-identical set regulates cell migration.

One key choice is whether to continue actin polymerization or to cap barbed ends with Capping protein. Enabled (Ena)/VASP family proteins bind barbed ends and prevent Capping protein binding, allowing continued filament elongation (Barzik et al., 2005; Bear et al., 2002) (see also Samarin et al., 2003). Ena/VASP proteins regulate cell migration in cultured mammalian fibroblasts, which predominantly produce lamellipodia (Bear et al., 2000; Bear et al., 2002). Inactivating Ena/VASP proteins triggered production of short, highly branched actin filaments within lamellipodia, driving more persistent lamellipodial protrusion that allowed cells to migrate faster than controls. Concentrating Ena/VASP proteins at the plasma membrane triggered production of long, sparsely branched actin filaments presumably lacking the strength to provide sustained force. Cells extended rapid but unstable lamellipodia and migrated more slowly than controls.

Ena/VASP proteins also influence filopodia (Mejillano et al., 2004), as was extensively studied in growth cones in culture (Lebrand et al., 2004), *Caenorhabditis elegans* axons (Chang et al., 2006) and Dictyostelium (Han et al., 2002). Growth cone motility shares features with cell migration (Dent and Gertler, 2003). Inactivating Ena/VASP in cultured neurons reduces growth cone filopodia, whereas concentrating Ena/VASP at the plasma membrane promotes filopodia (Lebrand et al., 2004). Interestingly, axon guidance defects are seen in zygotic loss-of-function Ena/VASP mutants in *Drosophila* (Bashaw et al., 2000; Gertler et al., 1995; Wills et al., 1999), *C. elegans* (Chang et al., 2006; Gitai et al., 2003; Shakir et al., 2006; Withee et al., 2004; Yu et al., 2002) and mice (Lanier et al., 1999; Menzies et al., 2004). *Dictyostelium* DdVASP also promotes filopodia (Han et al., 2002).

Ena/VASP proteins also localize to cell-cell adherens junctions (AJs) in flies (Baum and Perrimon, 2001; Grevengoed et al., 2001) and mammals, and are implicated in AJ formation in cultured keratinocytes (Vasioukhin et al., 2000) and mammary cells (Scott et al., 2006). This suggests that Ena/VASP proteins may play essential roles in cell adhesion. Finally, Ena/VASP proteins localize to cell-matrix junctions, perhaps underlying the role of VASP in platelet adhesion (reviewed by Krause et al., 2003).

As yet, no one has assessed the consequences of completely eliminating Ena/VASP function in mammals or flies. The three mammalian proteins (Mena, VASP and Evl) complicate analysis. *Mena* mutants have relatively subtle defects in forebrain commissures whereas *VASP* mutants have altered platelet aggregation (reviewed by Krause et al., 2003). *Mena;VASP* double mutants have more severe central nervous system (CNS) and craniofacial defects (Menzies et al., 2004). In *Drosophila*, loss of zygotic Ena disrupts axon guidance, but no one has removed maternal and zygotic Ena. Surprisingly, *C. elegans* Ena (*unc-34*)-null mutants are viable, without obvious effects in morphogenesis,

[1]Lineberger Comprehensive Cancer Center and Department of Biology, University of North Carolina at Chapel Hill, Chapel Hill, NC 27599, USA. [2]Department of Biology, Bucknell University, Lewisburg, PA 17837, USA. [3]Department of Cell Biology and Program in Neuroscience, Harvard Medical School, Boston, MA 02115, USA. [4]Massachusetts Institute of Technology, Department of Biology, Cambridge, MA 02139, USA.

*Author for correspondence (e-mail: peifer@unc.edu)

Accepted 12 March 2007

but embryos double mutant for *unc-34* and the actin-regulator *WASP* have severe morphogenesis defects (Withee et al., 2004), suggesting that *C. elegans* Ena/VASP is important but alternate actin regulatory mechanisms can compensate.

Ena/VASP proteins share several regions important for actin regulation (reviewed by Krause et al., 2003). The N-terminal EVH1 domain recognizes the sequence D/EFPPPPXD/E (FP4) (Ball et al., 2002) in Ena/VASP partners including zyxin, Robo receptors and Lamellipodin/RIAM, positioning Ena/VASP proteins at sites where their actin-regulatory activities are needed. The high affinity of EVH1 for its ligands allowed the Gertler laboratory to design a novel strategy to manipulate Ena/VASP function. They fused four FP4 motifs to a mitochondrial localization signal (FP4mito). This recruits Ena/VASP proteins from their normal cellular locations to mitochondria, effectively inactivating them and mimicking phenotypes of Ena/VASP-deficient fibroblasts and neurons (Bear et al., 2000; Bear et al., 2002; Lebrand et al., 2004). The C-terminal EVH2 domain binds G- and F-actin and mediates tetramerization. The central proline-rich region binds Profilin and SH3/WW-domain proteins, including Src and Abelson (Abl) kinases. Two point mutations affecting the CNS function of Ena in *Drosophila* were characterized (Ahern-Djamali et al., 1998). ena^{210} encodes a missense change in the EVH1 domain (A97V), blocking interaction with zyxin in vitro. ena^{23} truncates Ena in the EVH2 domain, blocking tetramerization but not G- or F-actin binding.

We seek to understand how cells use different tools in the actin regulatory toolkit to perform the diverse behaviors of development. We present the first assessment outside *C. elegans* of embryonic morphogenesis in the total absence of Ena/VASP function.

MATERIALS AND METHODS

Fly work

Mutations are described at flybase.bio.indiana.edu. DNAs encoding FP4mito-, AP4mito-, FP4CAAX- or AP4CAAX-EGFP fusion proteins were cut from the retroviral vector pMSCV (Bear et al., 2000) using *Eco*RI and *Hin*dIII, subcloned into pSTBlue-1, cut out with *Bam*HI and *Xba*I and subcloned into the P-element vector pUASg under the control of a Gal4-driven UAS promoter (Brand and Perrimon, 1993). The *ena* open reading frame (ORF) with an N-terminal green fluorescent protein (GFP)-fusion was also subcloned into pUASg. Stocks to generate *ena* germline clones and GAL4 drivers were from the Bloomington *Drosophila* Stock Center. UAS-GFPactin or RFPactin were from P. Martin (University College London, UK). *ena* germline clones were generated by heat-shocking 48-72 hour $hsflp^{12}$; FRT42B *ena*/FRT42B ovo^{D1} larvae for 3 hours at 37°C. Cuticle preparations were as in Wieschaus and Nüsslein-Volhard (Wieschaus and Nüsslein-Volhard, 1986).

Immunolocalization and microscopy

S2 and D16-C3 cells were cultured and plated as in Rogers et al. (Rogers et al., 2002) (with 10 μg/mL human insulin added for D16-C3), transfected, fixed and stained by the actin protocol in Rogers et al. (Rogers et al., 2004). For RNA interference (RNAi), D16-C3 cells were plated in six-well plates to 75% confluency and treated with 0.5 mL 20 μg/mL dsRNA for 30 minutes, followed by 1.5 mL growth medium on days 1 and 4; on day 7 cells were resuspended by pipetting and applied to acid-washed coverslips for 5 minutes. Embryos were fixed as in Grevengoed et al. (Grevengoed et al., 2001). Wing discs were fixed for 20 minutes in 4% formaldehyde on ice. All were blocked/stained in PBS/1% goat serum/0.1% Triton X-100 and mounted in Aqua-Polymount (Polysciences). Antibodies: mouse anti-Ena5G2 (1:500), anti-BP102 (1:200); anti-ArmN27A1 (1:200) and rat anti-DE-cadherin (DE-cad) (DCAD2, 1:200; all from the Developmental Studies Hybridoma Bank). Mitochondria were visualized by 45 minutes of incubation in 100 nm MitoTracker® Deep Red 633 (Invitrogen), and actin with Alexa Fluor-568-phalloidin. Secondary antibodies: Alexa Fluor-488, Alexa Fluor-568 and Alexa Fluor-647 (Invitrogen). Most images were acquired with an LSM510 confocal microscope (Carl Zeiss MicroImaging), LSM510AIM acquisition software and 40× (1.3 NA) or 63× (1.4 NA) objectives. D16-C3 cell images were acquired using a 100× (1.45 NA) objective, a TE2000-E inverted microscope (Nikon) and a CoolsnapHQ CCD camera (Roper Scientific). Brightness and contrast were adjusted in Adobe Photoshop® 7.0; alterations were performed identically on comparable wild-type and mutant images. Time-lapse imaging was as in Grevengoed et al. (Grevengoed et al., 2001). Images were captured every 5 seconds or 15 seconds. MetaMorph 6.1 (Molecular Devices, Union City, CA) was used to enhance brightness and contrast. Modifications were made on entire panels.

RESULTS

FP4mito sequesters Ena at mitochondria, phenocopying *ena* loss-of-function

To examine how loss and gain of Ena function affects morphogenesis, we developed tools to manipulate Ena function at particular times and places. This built on the Gertler laboratory sequestration strategy, using FP4 Ena-binding sequences to recruit Ena/VASP to mitochondria, effectively blocking function. We adapted this to *Drosophila*, generating an FP4mito fusion protein (Fig. 1A) controlled by a Gal4-driven UAS promoter. When introduced into cultured *Drosophila* S2 cells or used to generate transgenic flies, FP4mito dramatically alters endogenous Ena localization (Fig. 1B-C). In normal S2 cells (Fig. 1B′, asterisk), Ena is diffusely cytoplasmic, and concentrates at the leading edge (arrowhead), cell contacts (white arrow) and in punctate perinuclear structures. GFP-FP4mito colocalizes with a mitochondrial marker (Fig. 1B″-B‴, yellow arrows), and completely relocalizes Ena to mitochondria (Fig. 1B′, yellow arrow). In embryonic epidermis, Ena is diffusely cytoplasmic and concentrated at the amnioserosal cell cortex (Fig. 2L′, white arrow) and leading-edge AJs (Fig. 2L′, arrowhead). In embryos FP4mito recruits all detectable Ena to mitochondria, as judged by Ena/GFP-FP4mito colocalization (Fig. 2L,L′, blue arrows).

As a specificity control we generated flies expressing a mito construct with the conserved phenylalanine in each FP4 motif replaced by alanine (AP4mito). AP4mito recruited significantly less Ena (Fig. 2M,M′), although we saw occasional weak Ena recruitment (data not shown). As a second specificity control we expressed FP4mito throughout the epidermis in *ena* loss-of-function mutants. This did not change the severity or frequency of embryonic phenotypes (data not shown), suggesting that FP4mito does not have substantial off-target effects. Finally, we examined whether FP4mito alters WASP localization (WASP has an EVH1-like WH1 domain) – as expected, it does not (Fig. 1C-C″), consistent with known differences in binding specificities of WASP WH1 and Ena/VASP EVH1 (Volkman et al., 2002; Zettl and Way, 2002). Other EVH1-domain proteins such as Homer/VESL are similarly unlikely to bind as they recognize sequences in which the aromatic residue follows the prolines (Beneken et al., 2000; Barzik et al., 2001).

To verify that FP4mito inactivates *Drosophila* Ena, we expressed FP4mito in the CNS and peripheral nervous system (PNS) where the function of Ena is clear (reviewed by Krause et al., 2003). CNS longitudinal axons extend parallel to the midline (Fig. 1D, arrowhead) and commissural axons cross it (Fig. 1D, arrow). FP4mito-expressing embryos have reduced longitudinal axons (Fig. 1E,G, arrowheads), resembling zygotic *ena* mutants in the range and severity of defects (Fig. 1F,H; see Table S1 in the supplementary material) (Bashaw et al., 2000). To further assess FP4mito specificity we expressed it zygotically in *ena* zygotic mutants – this

did not increase severity of CNS defects (see Table S1 in the supplementary material), consistent with FP4mito specifically affecting Ena. We also sequestered Ena at mitochondria in the PNS. Motor axon projections of intersegmental nerve b (ISNb) normally turn toward their muscle targets (Fig. 1I, left; Fig. 1J). In zygotic *ena* mutants ISNb axons fail to turn, continuing toward inappropriate targets (Fig. 1I, right) (Wills et al., 1999). This bypass phenotype is seen in 88% of segments when FP4mito is expressed using *elav*-Gal4 (n=86; Fig. 1K,L); this is quantitatively comparable to zygotic *ena* loss-of-function (79-96%) (Wills et al., 1999). AP4mito expression using *elav*-Gal4 (Fig. 1J) did not cause significant ISNb bypass (2% of segments, n=150; like wild type). Thus, removing Ena from its normal location and sequestering it at mitochondria effectively blocks Ena function in intact animals. By contrast, FP4CAAX, which in cultured fibroblasts activates Ena by recruitment to the plasma membrane (Bear et al., 2000), had no effect on CNS axons (data not shown) or ISNb guidance (Fig. 1N), consistent with previous analysis of Ena overexpression (Wills et al., 1999). Expressing the control AP4CAAX in the PNS also had no effect (Fig. 1M).

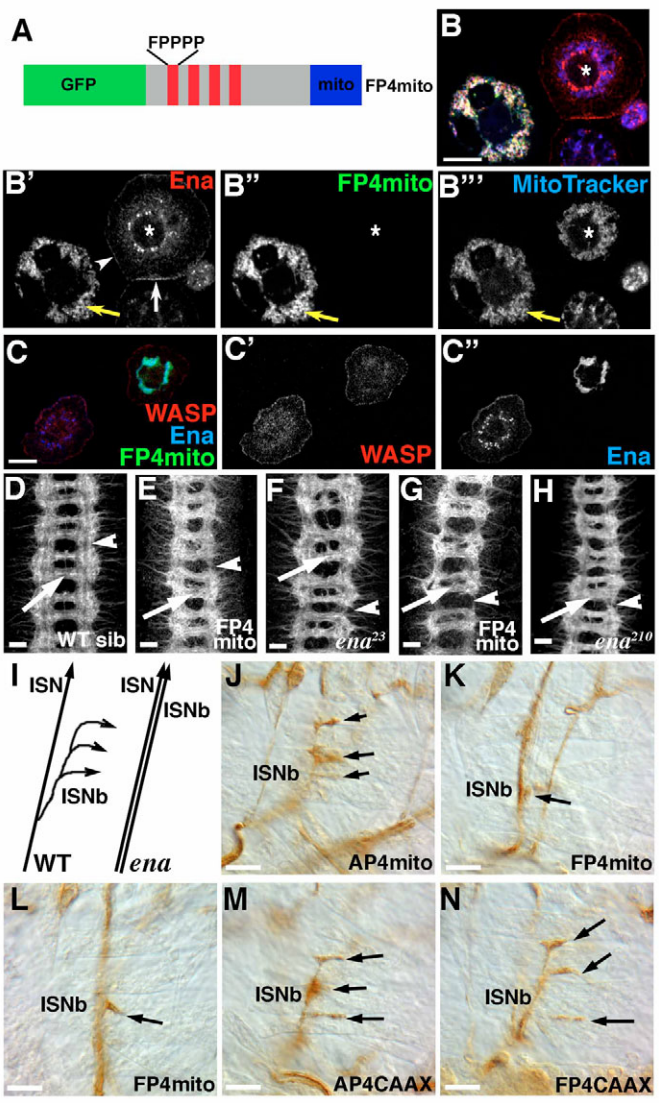

Fig. 1. FP4mito alters Ena localization and phenocopies *ena* loss-of-function. (**A**) FP4mito. (**B-C″**) S2 cells, antigens indicated. (B) In wild-type cells (asterisk), Ena is diffusely cytoplasmic and enriched at leading edge (arrowhead) and cell contacts (white arrow). In FP4mito-expressing cells, GFP-FP4mito colocalizes with MitoTracker and Ena (yellow arrow). (C) FP4mito does not recruit WASP. (**D-H**) Embryonic CNS, BP102 antibody. (D) Control. (E,G) FP4mito × e22c-Gal4. (F) ena^{23}/ena^{GC1}. (H) ena^{210}/ena^{GC1}. Longitudinal (arrowhead) and commissural axons (arrow). (**I**) ISNb motor axon projections; wild type (left), *ena* mutants (right). (**J-N**) Projections of ISNb (arrows, anti-Fasciclin II) in embryos expressing indicated constructs (*elav*-Gal4). Scale bars: 10 μm.

Dynamic localization of Ena

Ena localizes to AJs and the cytoplasm, from after cellularization (Fig. 2A, inset), through gastrulation (Fig. 2A) and into the extended germband stage (Fig. 2B,C). After germband extension, Ena remains at AJs and concentrates at epidermal tricellular junctions (Fig. 2C, arrowheads); it is uniformly localized around the amnioserosal cell cortex (Fig. 2C,D, arrows; Fig. 2G). During dorsal closure Ena becomes concentrated along the front of leading-edge cells (Fig. 2D′, arrowhead), becoming strongly enriched in spots at leading-edge AJs (Fig. 2E-G, arrowheads), but remaining at tricellular junctions (Fig. 2D′,E,G, blue arrowheads). Ena is especially enriched in the single row of cells per segment that initiate segmental grooves (Larsen et al., 2003) (Fig. 2F,G, arrows) and in cells at the anterior edge of the dorsal-fold (Fig. 2H,I, arrows) that lead during head involution.

Ena plays several roles during morphogenesis

To determine whether Ena is required for epithelial architecture or morphogenesis, we inactivated maternal and zygotic (M/Z) Ena using two approaches that each should cause strong loss-of-function. First, we expressed FP4mito in the germline using matα4-Gal4-VP16 (matGal4; mat-FP4mito), so that FP4mito was loaded into eggs [only 8% of mat-FP4mito eggs are fertilizable (n=400), because of the roles of Ena during oogenesis; our unpublished data]. Although no zygotic Gal4 is produced, maternal FP4mito remained throughout embryogenesis, effectively sequestering zygotic and maternal Ena from cellularization (see Fig. S1J,K in the supplementary material) through dorsal closure and later (Fig. 3A versus Fig. 3B,C). No Ena was detectable at its usual locations, even in places in which it accumulates to high levels, such as leading-edge cell AJs (Fig. 3A versus Fig. 3C, arrows), so this should be a very strong to complete loss of maternal and zygotic function. Second, we generated females with germlines mutant for the very strong loss-of-function ena^{23} allele or the strong ena^{210} allele (allele strength assessed in the PNS) (Wills et al., 1999), and crossed them to males heterozygous for the null allele ena^{GC1}; half the embryos are M/Z*ena* mutant. In M/Zena^{23} mutants selected using a GFP-marked balancer, Ena protein levels were significantly reduced and no localized protein was seen (Fig. 3D″ versus Fig. 3E″). Neither ena^{23} nor ena^{210} is protein null (Ahern-Djamali et al., 1998), but attempts to generate germline clones with the protein-null allele ena^{GC1} failed, perhaps because it results from a chromosomal inversion.

The cuticle secreted by epidermal cells provides a simple means to assess morphogenesis defects. More than 70% of zygotic *ena* mutants are wild type, whereas ~20% display misalignment/puckering along the dorsal midline, indicating late dorsal closure defects. Ubiquitous zygotic FP4mito expression has similar effects (Fig. 4A,J versus Fig. 4B,K, arrowheads). By contrast, 79% of mat-FP4mito embryos die, and both mat-FP4mito embryos and M/Zena^{23} mutants disrupt several morphogenetic processes [the control matGal4-AP4mito is not embryonic lethal (1%, n=586)]. Eighty to ninety per cent of mat-FP4mito or M/Zena^{23} mutants have

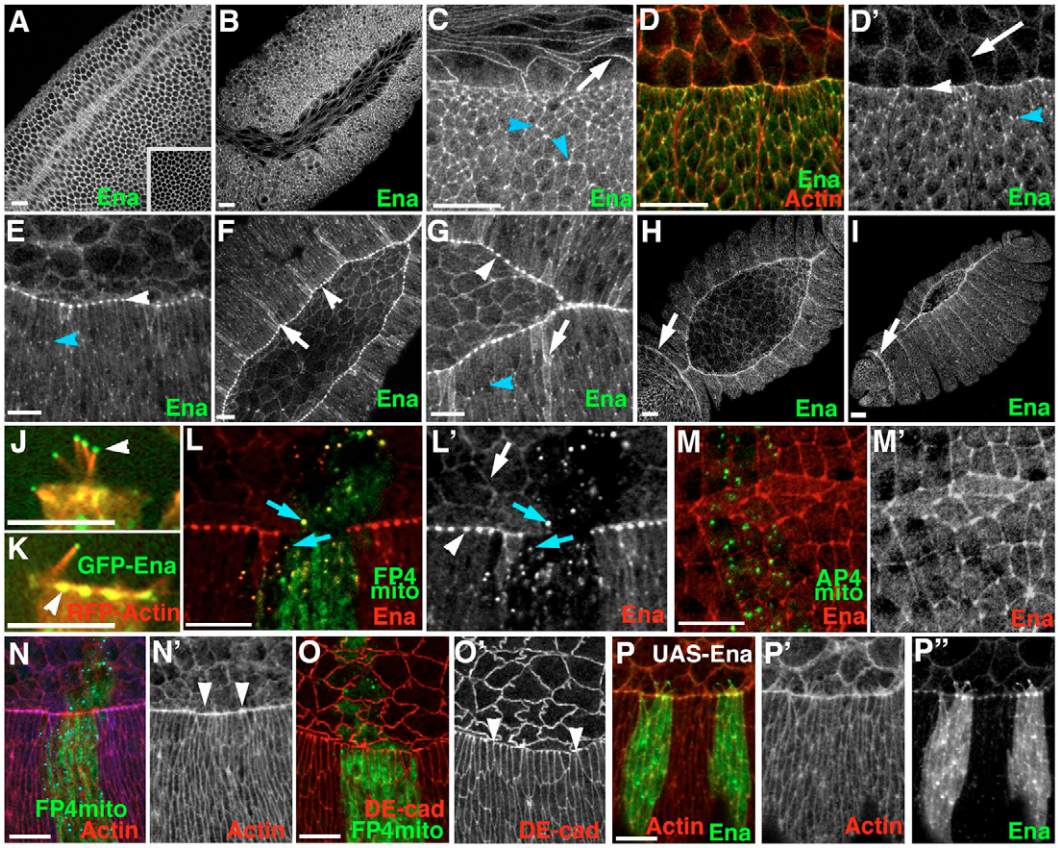

Fig. 2. Ena localization. Wild-type embryos, anterior left, antigens indicated. (**A**, inset) Cellularization, surface view. (A) Gastrulation, ventral view. (**B-D**) Stages 10 and 12. Arrows, amnioserosa; blue arrowheads, tricellular junctions. White arrowhead in **D′**, leading edge. (**E**,**H**) Onset of dorsal closure, (**F**,**G**,**I**) mid-late dorsal closure: arrowheads, Ena at leading-edge AJs; blue arrowheads, tricellular junctions. Arrows in F,G, segmental groove cells; arrows in H,I, dorsal-fold. (**J**,**K**) Live embryos. GFP-Ena at filopodial tips (J, arrowhead) and leading-edge AJs (K, arrowhead). (**L**,**L′**) FP4mito (*paired*-Gal4). FP4mito recruits Ena from cytoplasm and AJs to punctate structures (blue arrows). Adjacent wild-type cells retain Ena at amnioserosal cell cortex (white arrow) and leading edge AJs (arrowhead). (**M**) AP4mito (*engrailed*-Gal4) does not recruit Ena. (**N**,**O**) FP4mito (green, *paired*-Gal4). (**N′**,**O′**) Expression boundaries (arrowheads). Unaltered cortical actin and actin/myosin cable (N), DE-cad (O). (**P**) UAS-Ena (*engrailed*-Gal4) elevates Ena levels (**P″**) without altering cable or cortical actin (**P′**). Scale bars: 20 μm.

defects in head involution, disrupting head cuticle (Fig. 4D, arrow). To our surprise, dorsal closure was completed, but embryos have dorsal midline defects like those of *ena* zygotic nulls (Fig. 4B,D,G, arrowheads). A subset of embryos exhibited ventral epidermal defects (Fig. 4H). Two differences were apparent between mat-FP4mito and M/Z*ena*^{23}. M/Z*ena*^{23} mutants did not exhibit germband retraction defects, but their ventral epidermal defects were more frequent. M/Z*ena*^{210} mutants were similar to, but significantly less severe, than M/Z*ena*^{23} (Fig. 4).

Disrupting Ena function does not affect cellularization or epithelial integrity

We next examined the cell biological consequences of Ena inactivation. Flies initiate embryogenesis with 13 syncytial nuclear divisions; during interphase actin forms microvillar caps over nuclei, whereas during mitosis it lines transient pseudocleavage furrows separating spindles. Inappropriate apical Ena triggered by inactivating Abl kinase disrupts furrows, increasing microvillar actin and reducing actin in pseudocleavage furrows (Grevengoed et al., 2003).

By contrast, maternal *ena*^{23} mutants form a normal cellular blastoderm without large-scale defects in pseudocleavage furrows or cellularization (see Fig. S1C,D,L in the supplementary material). Many mat-FP4mito early embryos were also roughly normal (see Fig. S1E,F in the supplementary material), although some embryos had elevated nuclear loss (see Fig. S1G,H, arrows, in the supplementary material), a defect we also saw in some maternal *ena*^{23} mutants. This may be because of loss of maternal Ena, or may result from oogenesis defects. A subset of mat-FP4mito embryos had major defects in nuclear distribution and actin at the anterior end (see Fig. S1I in the supplementary material). We observed similar defects in *arm*^{XP33} maternal mutants that disrupt nurse cell dumping during oogenesis (Cox et al., 1996). We thus think it likely that these defects are indirect consequences of oogenesis defects in mat-FP4mito mothers. mat-FP4mito embryos are also smaller than wild type, probably because of defects in nurse cell dumping (data not shown).

Ena plays an important role in adhesion and cortical actin in cultured keratinocytes, mammary cells and *Drosophila* follicle cells (Baum and Perrimon, 2001; Vasioukhin et al., 2000; Scott et al., 2006). We thus examined epithelial integrity in M/Z*ena*^{23} and mat-FP4mito embryos. Both proceed through gastrulation normally (Fig. 5A-D). Epithelial integrity is normal with no detectable change in *Drosophila* E-cadherin (DE-cad), Armadillo, alpha-catenin (Fig. 2O; Fig. 5I versus Fig. 5J; data not shown) or cortical actin (Fig. 2N, Fig. 5E-H). Thus, disrupting Ena function does not disrupt AJs or

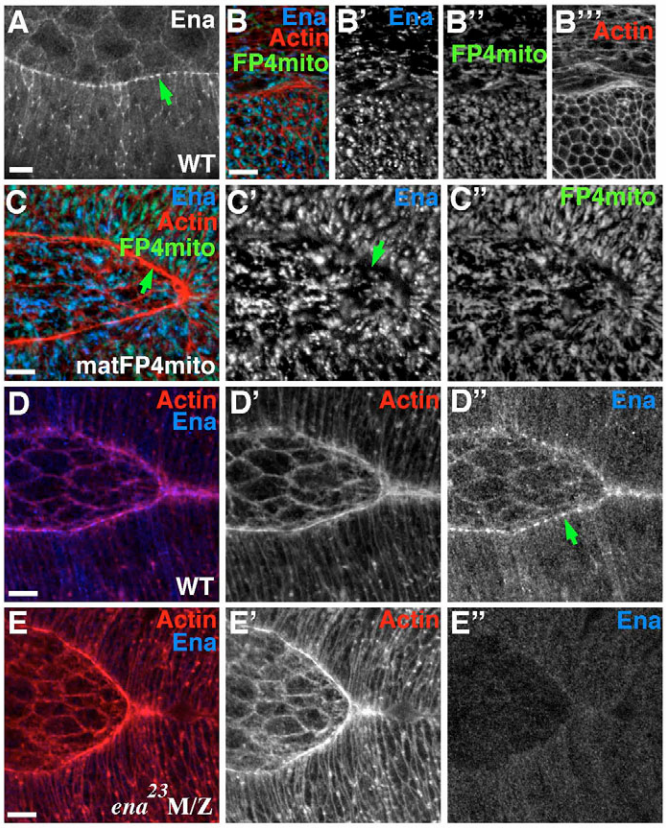

Fig. 3. Both FP4mito and *ena*^{23} disrupt Ena localization. (**A**) Wild-type Ena, stage 13. (**B-C″**) mat-FP4mito, stages 10 and 13. Mislocalized Ena. (**D-E″**) Stage 13 wild type and M/*Zena*^{23}. Arrows, AJs of leading-edge cells. Scale bars: 10 μm.

epithelial integrity. To assess whether embryonic epithelia are the exception, we disrupted Ena function in posterior cells of larval imaginal discs (FP4mito × *engrailed*-Gal4), a polarized, folded epithelium with actin and DE-cad at apical AJs (see Fig. S1N,O in the supplementary material). FP4mito relocalized Ena to presumptive mitochondria (see Fig. S1M, arrowheads, in the supplementary material), with no detectable effect on epithelial architecture, cortical actin or DE-cad (see Fig. S1N,O in the supplementary material). We also generated clones of *ena*^{23} mutant cells, which did not affect actin or epithelial architecture (data not shown). Thus, Ena is not essential for epithelial architecture or actin organization in embryos or imaginal discs.

Ena plays important roles in morphogenesis

Germband extension, ventral furrow formation and posterior midgut invagination occurred normally in M/*Zena*^{23} mutants and mat-FP4mito embryos. The first defects occurred during germband retraction, when epidermal and amnioserosal cells move together as a coherent sheet. This movement is thought to be driven by a dramatic shortening of amnioserosal cells along their dorsal/ventral axis, assisted by extension of epidermal cells along their dorsal/ventral axis (Schock and Perrimon, 2002). This requires stable connections between amnioserosa and epidermis, achieved in part by large amnioserosal lamellipodia extending over the posterior-most epidermal cells. βPS-integrin mutants fail to form stable lamellipodia; when amnioserosal cells change shape, they detach from posterior epidermal cells, disrupting germband retraction (Schock and Perrimon, 2003). Approximately 40% of mat-FP4mito embryos failed to complete germband retraction (Fig. 4E), and had defects in attachment of amnioserosa and epidermal cells. Although amnioserosal detachment is most obvious after retraction begins (Fig. 5O,P versus Fig. 5M,N, arrows), prior to germband retraction there is less overlap of amnioserosal cells and posterior epidermis (Fig. 5K versus Fig. 5L, brackets). As a result, while amnioserosal cells change shape, germband retraction fails (Fig. 5O,P).

M/*Zena*^{23} and mat-FP4mito embryos also have major defects in segmental furrow retraction. Ena has a striking localization in segmental groove cells (Fig. 2F,G), which apically constrict at the onset of germband retraction and migrate inwards, pulling in neighbors on either side (Larsen et al., 2003). Segmental grooves persist ventrally and dorsally through early dorsal closure, regressing by its completion; grooves remain longest laterally (Fig. 6E, arrowheads). M/*Zena*^{23} (Fig. 6B,D,H, arrowheads) and FP4mito segmental grooves (Fig. 6F,M, arrowheads) are deeper than wild type and persist long after they should have regressed (Fig. 6T,U, arrowheads; Fig. 6S). The leading edge during dorsal closure is often uneven in M/*Zena*^{23} and FP4mito (Fig. 6B,M), perhaps in part because of overly deep grooves.

Shortly after germband retraction, head involution begins, with ectoderm migrating anteriorly driven by coordinated cell shape changes. Most M/*Zena*^{23} mutants and mat-FP4mito embryos fail in this process (Fig. 6S,T,X, brackets), leading to the head holes seen in cuticles (Fig. 4C,D, arrows). Cells that should lead head involution appear to constrict far more than in wild type, nearly severing the head from the thorax (Fig. 6S,X).

Ena localization in filopodia

Among the most dramatic morphogenetic events is dorsal closure, in which lateral epidermal sheets move toward one another, meet and fuse at the dorsal midline, enclosing embryos in epidermis. This is driven by several forces, including leading-edge actin/myosin cable contraction, amnioserosal cell apical constriction and dorsal/ventral elongation of epidermal cells (Kiehart et al., 2000; Hutson et al., 2003). Ena is concentrated at leading-edge AJs (Fig. 2E-G, arrowheads), where the actin cable is anchored, and leading-edge cells exhibit highly dynamic actin protrusions while migrating (Jacinto et al., 2000). This suggested that Ena might play a key role in dorsal closure.

As dorsal closure begins, leading-edge cells produce lamellipodia and filopodia (Jacinto et al., 2000). In live embryos, GFP-Ena concentrated at tips of leading-edge filopodia (Fig. 2J, arrowhead) and at leading-edge AJs (Fig. 2K, arrowhead). Although filopodia are not generally preserved after fixation, they were easily visualized in fixed embryos overexpressing Ena (Fig. 2P). We did not observe GFP-Ena concentration at the lamellipodial leading edge, but high levels of GFP-Ena in AJs may obscure this. GFP-Ena also accumulated in intracellular puncta that may be overexpression aggregates, but these do not substantially disrupt cell function as pan-epidermal GFP-Ena expression is not embryonic lethal (e22c-GAL4; 1% lethality, *n*=294).

GFP-Ena allowed us to examine the localization of Ena within leading-edge filopodia as they extend and retract. Consistent with the anti-capping role of Ena, GFP-Ena concentrated at tips of extending filopodia (Fig. 7A, arrow). Remarkably, GFP-Ena is retained at filopodial tips as they retract (Fig. 7B, arrow; see Movie 1 in the supplementary material). GFP-Ena particles move away from filopodial tips before they retract (Fig. 7B, arrowhead; see Movie 1 and Fig. S2 in the supplementary material), with some

GFP-Ena remaining at tips during initial retraction. Rearward movement of GFP-Ena continues as retraction proceeds and tip-associated GFP-Ena usually eventually disappears.

During dorsal closure, filopodia usually form from lamellipodia, but what triggers filopodial formation is not clear. Insight came from embryos expressing both GFP-actin and GFP-Ena, in which leading-edge cells produce large lamellipodia containing numerous actin microspikes (Fig. 7C). Over time a subset of microspikes merge at their distal ends to produce filopodia (Fig. 7C; see Movie 2 in the supplementary material). Similar events were observed in embryos overexpressing untagged Ena (Fig. 9D, 5:04-7:04, arrow).

Inactivating Ena slows epithelial zippering and impedes cell matching

We hypothesized that Ena would play a key role in dorsal closure, modulating actin cables or helping drive migration. However, both mat-FP4mito and M/Z*ena*^{23} mutants complete dorsal closure with levels and localization of DE-cad (data not shown) and cortical actin (Fig. 6I-L) in amnioserosa and epidermis indistinguishable from wild type, and with a largely normal actin/myosin cable (Fig. 6I versus Fig. 6J,L, arrows). Amnioserosal apical constriction and epidermal cell elongation (Fig. 6J-L, arrowheads; Fig. 6O versus Fig. 6P) are usually normal, although occasional cells have splayed open (Fig. 6J,L, brackets) or hyperconstricted leading edges. In a few embryos many epidermal cells fail to change shape (Fig. 6N, arrowheads). These defects do not block completion of dorsal closure, but Ena inactivation disrupts cell matching along the dorsal midline (Fig. 6W versus Fig. 6V). FP4mito expression in stripes in each segment (*engrailed*- or *paired*-Gal4) also did not affect cortical actin or the actin/myosin cable (Fig. 2N′, between arrowheads).

To examine the role of Ena during dorsal closure more closely, we inactivated it throughout the epidermis and amnioserosa (FP4-mito × e22c-Gal4). This caused embryonic lethality (85%, *n*=163; versus AP4mito lethality=1%, *n*=147), and disrupted cell matching at the midline (Fig. 4A,J versus Fig. 4B,K, arrowheads), similar to *ena* zygotic mutants. In fixed embryos we observed deep segmental grooves and an uneven leading edge (data not shown), as in M/Z*ena*^{23} mutants. We examined dorsal closure in real time in embryos expressing FP4mito and GFP-actin using e22c-Gal4. This revealed severe abnormalities in epithelial zippering; dorsal openings were oval rather than almond-shaped (Fig. 8A versus Fig. 8B) and leading edges sometimes met in the middle before zippering occurred (Fig. 8B, 62:42, arrow). As a result, migration was 2.2-fold slower than wild type ($P=2\times10^{-7}$), with much of the delay in late epithelial zippering (Fig. 8; see Movies 3, 4 in the supplementary material).

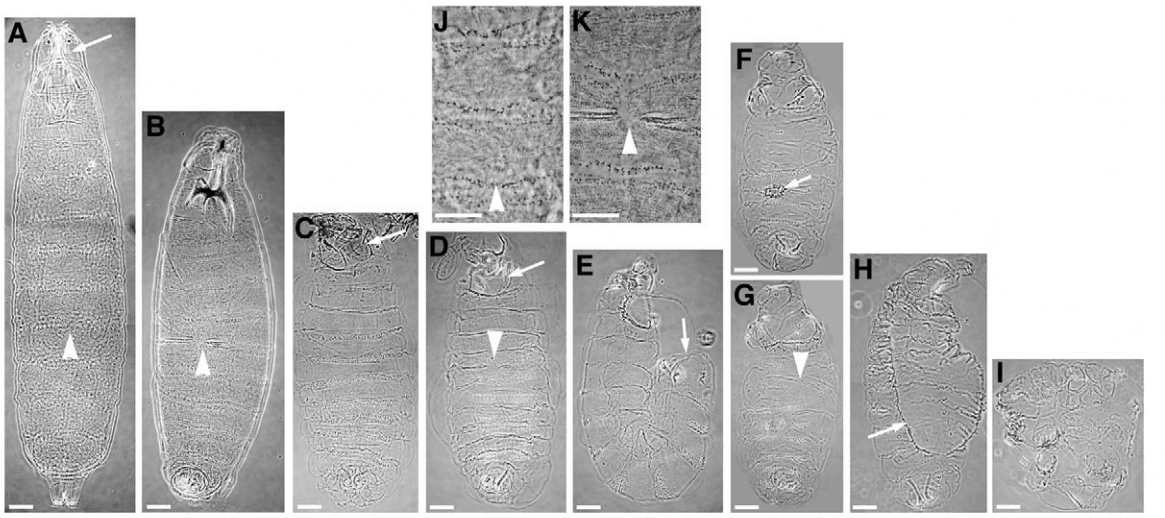

	wild type	dorsal pucker	head hole	head hole and pucker	germband retraction	head, ventral holes	large ventral hole	no ventral cuticle	N
ena^{23} m/z	8%	10%	37%	15%	0%	0%	28%	2%	137
ena^{210} m/z	27%	15%	36%	14%	0%	0%	7%	1%	160
matGal4-FP4mito	1%	8%	18%	22%	39%	3%	6%	3%	170
ena^{23} zyg	74%	21%	5%	0%	0%	0%	0%	0%	211
ena^{210} zyg	78%	17%	4%	0%	0%	0%	1%	0%	215
e22c-Gal4-FP4mito	68%	30%	2%	0%	0%	0%	0%	0%	142
ena$^{GC5/GC1}$ =zyg null	75%	21%	2%	0%	0%	1%	0%	0%	326

Fig. 4. Ena is essential for morphogenesis. Cuticles. Wild-type (**A**,**J**) and representative *ena* mutant (**C**,**H**,**I**) or FP4mito-expressing (**B**,**D-G**,**K**) embryos illustrating phenotypic classes. (J,K) Close-ups of A,B. Arrowheads, wild type (A,J) or defective dorsal midline (B,D,G,K). Arrows in A,C,D, wild type (A) or failed head involution (C,D). Arrow in E, germband retraction failure. Arrows in F,H, small or large ventral holes. Bottom, frequency of defects for each genotype. Scale bars: 100 μm.

Inactivating Ena disrupts filopodia

We next examined how Ena inactivation affects actin-based protrusions. Wild-type leading-edge cells produce protrusions resembling growth cones, with filopodia arising from lamellipodia (Fig. 9A, arrows; see Movie 5 in the supplementary material). We expressed GFP-actin and FP4mito together, using *engrailed*-Gal4, allowing us to monitor leading-edge protrusions when Ena is inactivated. The results were striking. FP4mito-expressing leading-edge cells produce lamellipodia (Fig. 9B; see Movie 6 in the supplementary material), but produce only rare, very short filopodia (Fig. 9B, 4:00, arrow). We measured the number and maximum length of filopodia (any thin protrusion extending beyond the lamellipodium or leading edge within one-half of an *engrailed* stripe in 3-4 embryos/genotype as leading edges moved from 23.6 μm to 10.9 μm apart, using a defined distance rather than a defined time as FP4mito-expressing embryos close more slowly). Wild-type cells produce an average of 58 filopodia, with maximum length averaging 2.18 μm. FP4mito expression reduces both filopodial number and length (average filopodia number reduced from 58 to 20; average maximum length reduced from 2.18 μm to 1.16 μm; $P<0.0001$ for length and $P=0.013$ for number; these and other P values are via Student's t-test; Table 1; Fig. 9F), paralleling effects of inactivating Ena/VASP proteins in cultured neurons (Lebrand et al., 2004) or Dictyostelium (Han et al., 2002).

In fibroblasts FP4mito decreases rates of lamellipodial protrusion and retraction (Bear et al., 2002). We did not observe obvious effects of Ena inactivation on lamellipodia. Because wild-type protrusions combine lamellipodia and filopodia and new protrusions often form adjacent to or on top of existing ones, it is difficult to accurately follow a single lamellipodium through its lifecycle. Although lamellipodia of FP4mito-expressing cells can remain extended for several minutes (Fig. 9C), this is not substantially different from wild type.

Table 1. Number and maximum average length of filopodia produced over a fixed interval

	Average maximum length (μm)	Number of filopodia
Control embryo 1	2.08	67
Control embryo 2	2.12	32
Control embryo 3	2.85	51
Control embryo 4	1.86	81
Control embryos combined*	**2.18**	**58**
FP4mito embryo 1	1.34	12
FP4mito embryo 2	1.33	19
FP4mito embryo 3	0.92	25
FP4mito embryo 4	1.06	23
FP4mito embryos combined*	**1.12**	**20**
Ena overexpression embryo 1	2.51	120
Ena overexpression embryo 2	2.52	62
Ena overexpression embryo 3	2.55	90
Ena overexpression embryos combined*	**2.52**	**91**
FP4CAAX embryo 1	2.76	43
FP4CAAX embryo 2	2.94	73
FP4CAAX embryo 3	2.24	93
FP4CAAX embryos combined*	**2.60**	**70**

*Combined average lengths were calculated by adding the lengths of all filopodia from all embryos of a given genotype and dividing by the total number of filopodia. Combined average numbers were calculated by adding the number of filopodia for each embryo of a given genotype and dividing by the total number of embryos.

Ena promotes filopodial formation and elongation

Given the ability of Ena to promote filament elongation, we hypothesized that increasing Ena activity would increase filopodial number and/or length. Embryos overexpressing Ena produce longer filopodia than wild type (Fig. 9D; see Movie 7 in the supplementary material; average maximum length=2.52 μm versus 2.18 μm for

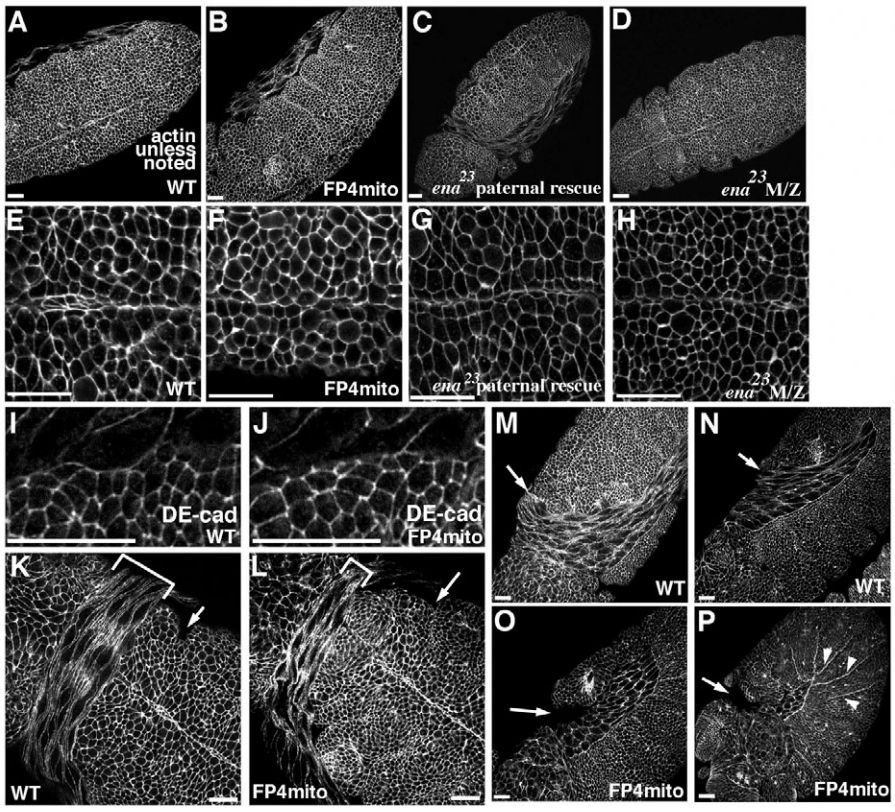

Fig. 5. Inactivating M/Z Ena does not disrupt cell adhesion. F-actin (except I,J, DE-cad). (**A-J**) Extended germband. mat-FP4mito and M/Z*ena*^{23}. Morphology (A-D), cortical actin (E-H) and DE-cad (I,J) normal. (**K**,**L**) Early germband retraction. mat-FP4mito (L) amnioserosal cells (brackets) do not overlap posterior epidermis (arrows) to the same extent as wild type (K). Smaller cell size in mat-FP4mito is probably because of overall smaller size of embryos, because of defects in nurse cell dumping. (**M**-**P**) Germband retraction. (M,N) Wild-type. Amnioserosa and epidermis maintain close contact throughout (arrows). (O,P) mat-FP4mito. Arrows, amnioserosa detached from epidermis. Arrowheads in P, deep segmental grooves. Scale bars: 20 μm.

wild type; *P*=0.0024; Table 1; Fig. 9F). Overexpressing Ena may also increase filopodial number: it increased to 91 filopodia versus 58 filopodia in wild type (Table 1), although this difference did not reach statistical significance in the sample size we quantitated. FP4CAAX, which should increase plasma membrane Ena activity, also promoted longer filopodia (average maximum length=3.00 μm versus 2.18 μm for wild type; *P*=0.0014; Table 1; Fig. 9E,F). Normally, filopodia are only produced by leading-edge cells, whereas lateral epithelial cells do not produce obvious protrusions. Interestingly, lateral epithelial cells overexpressing Ena produce many filopodia (Fig. 9G) on their lateral and apical surfaces. Thus, overexpressing Ena or concentrating it at the membrane both trigger longer filopodia and may promote de novo filopodial formation. Despite the dramatic effect on filopodia, dorsal closure is completed normally, and animals overexpressing Ena or expressing FP4CAAX ubiquitously (e22c-Gal4) complete embryogenesis and survive to adulthood.

Abl regulates Ena localization and filopodial formation

Multiple actin regulators play roles in filopodia, and in turn are regulated by signal transduction pathways. To begin to assess how Ena fits into this scheme, we examined proteins thought to antagonize or regulate Ena. Ena is thought to oppose Capping protein, and the tyrosine kinase Abl is an important Ena regulator. We first assessed Ena, Capping protein and Abl function in a model *Drosophila* cell line, D16-C3, derived from larval wing imaginal discs. When sparsely plated on polylysine, D16-C3 cells attach and assemble a halo of fine protrusions around their circumference (Fig. 10A). We believe these to be bona fide filopodia because: (1) they are actin-rich and morphologically resemble filopodia in their uniform diameter (Fig. 10A); (2) time-lapse imaging of cells expressing GFP-actin revealed cycles of protrusion, lateral movement and retraction (data not shown); and (3) they contain

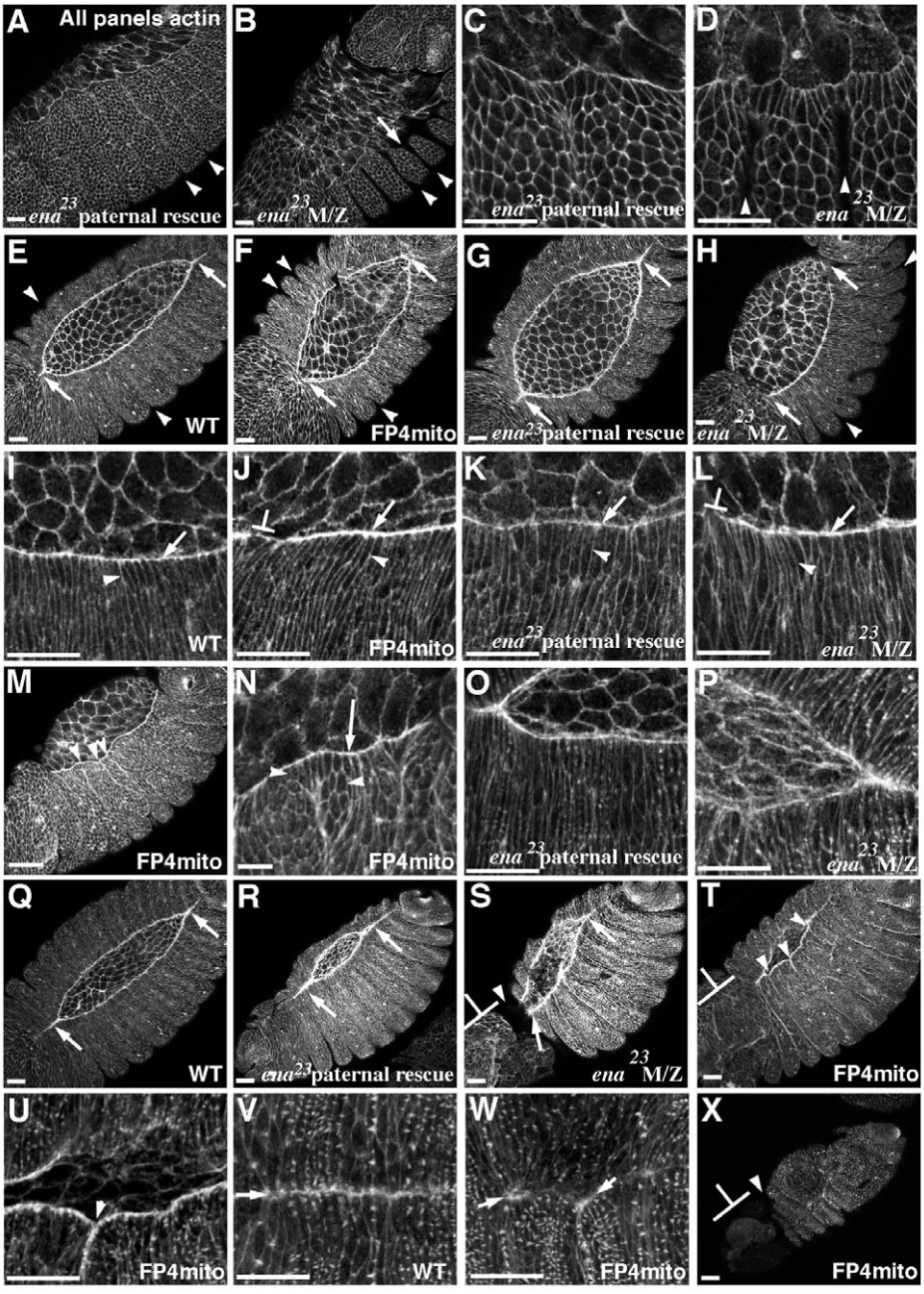

Fig. 6. Inactivating M/Z Ena disrupts morphogenesis. F-actin. (**A-D**) M/Z*ena*^{23}. Late germband retraction. Arrowheads, deep segmental grooves; arrow, uneven leading edge. (**E-N**) Onset of dorsal closure. (E-H) Deep segmental grooves (E-H, arrowheads). Arrows, failure of epidermal-zipping relative to wild type (E) or paternally rescued mutant (G). (I-L) Close-ups. Arrows, actin cable; arrowhead, cells elongating; brackets, occasional cells with disrupted actin cable and splayed-open leading edges. (M,N) More severely affected mat-FP4mito embryo. Note deep segmental grooves (M, arrowheads) and defects in cell-shape changes (N, arrowheads). Actin cable is largely normal (N, arrow). (**O-U**) Mid-late dorsal closure. Wild-type (Q), paternally rescued mutants (O,R), mat-FP4mito (T,U, close-up) and M/Z*ena*^{23} mutant (P,S). Note head involution failure (S,T, brackets), persistent deep grooves (T,U, arrowheads) and slow epidermal-zipping (Q-S, arrows). (**V**,**W**) End of dorsal closure. Arrows, dorsal midline. (**X**) Terminal-stage mat-FP4mito. Bracket, severe head defects. Scale bars: 20 μm.

molecules enriched in filopodia such as Ena (localized to tips; see below) and the actin cross-linker fascin (present along the length; data not shown).

We depleted Ena, Capping protein beta (CPB) and Abl from D16-C3 cells using RNAi and assessed filopodia formation and actin organization. In D16-C3 cells treated with control dsRNA (pBluescript), 91.5% of cells (n=320) elaborated filopodia. Following 7-day treatment with dsRNA to deplete Ena or CPB, staining with antibodies to each protein revealed significant reductions in protein levels (data not shown), consistent with our work in S2 cells in which these same reagents reduced protein levels to <5% relative to controls (Rogers et al., 2003). Ena depletion dramatically altered D16-C3 cell morphology, with most cells (94.5%, n=540 cells) lacking any detectable filopodia. Instead, Ena RNAi-treated cells exhibited a morphology dominated by lamellipodial protrusions (Fig. 10B). By contrast, CPB RNAi produced D16-C3 cells (91.3%, n=470 cells) with more numerous and longer filopodia (Fig. 10C). In addition, fluorimetric analysis revealed that, relative to control-treated cells (n>5000 cells), CPB RNAi increased mean F-actin levels by >160% (n>5000 cells) whereas in Ena-depleted cells F-actin remained unchanged. Therefore, CPB is a key regulator of actin polymer levels in these cells. To test the role of Abl in filopodia, we performed Abl RNAi. Consistent with a role for Abl as an Ena negative regulator (Gertler et al., 1995), Abl depletion resulted in a dramatic increase in filopodial length and number (Fig. 10D), and increased mean F-actin levels to 120% (n>5000 cells) over controls. We next assessed whether this occurred via effects on Ena localization. Filopodia in Abl RNAi-treated cells accumulated qualitatively higher Ena levels at filopodial tips than did control RNAi cells (Fig. 10E,F).

We next turned to embryos to examine whether Abl regulation was relevant to filopodia during dorsal closure. Wild-type filopodia are poorly preserved after fixation, and thus we are not often able to visualize them in wild-type embryos. However, Ena overexpression produced filopodia that were robust to fixation (Fig. 2P). To assess the role of Abl in filopodial regulation, we examined embryos maternally and zygotically mutant for the null allele abl^4 (M/Zabl), focusing on the leading edge during dorsal closure. In wild-type controls we saw strong Ena localization to leading-edge AJs as well as the amnioserosal cell cortex, but did not see obvious Ena localization at filopodial tips (Fig. 10I,J). By contrast, in M/Zabl mutants we saw numerous filopodia at the leading-edge terminating in prominent Ena dots (Fig. 10K,L, arrows). Furthermore, reducing Abl levels via *abl* heterozygosity reduced the phenotypic severity of zygotic Ena inactivation (FP4mito × e22c-Gal4; see Table S2 in the supplementary material). These data suggest that Abl negatively regulates filopodial formation by preventing Ena recruitment to forming filopodia. This is consistent with effects of overexpressing Abl in embryos, in which filopodia are significantly reduced (T. Stevens and M.P., unpublished).

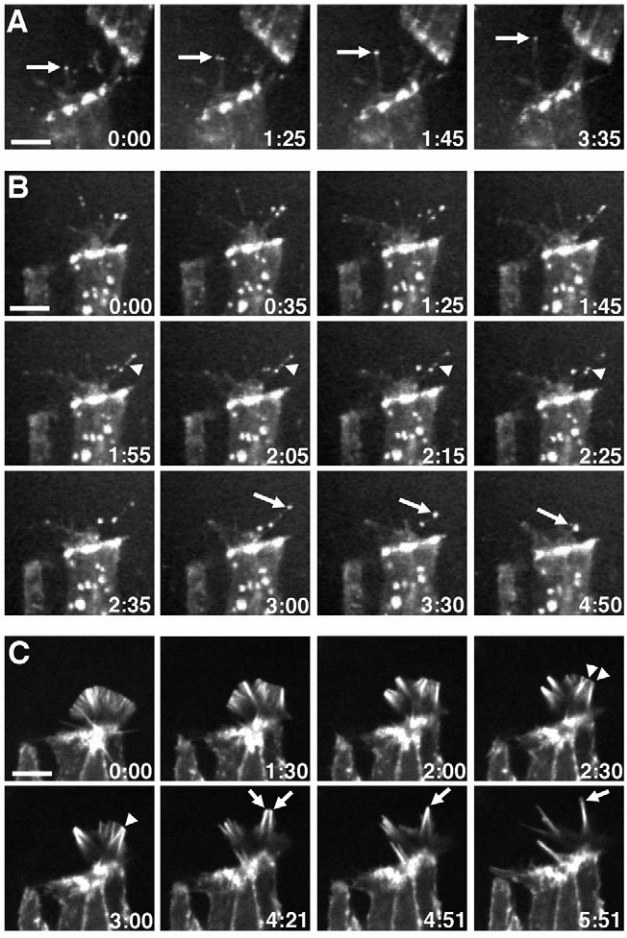

Fig. 7. GFP-Ena in filopodia. Movie stills showing embryos expressing GFP-Ena alone (**A**,**B**) or with GFP-actin (**C**) using *engrailed*-Gal4. Time, minutes:seconds. (A) GFP-Ena at filopodial tip as it extends (arrows). (B) See Movie 1 in thesupplementary material. Arrows, GFP-Ena remains at filopodial tip during retraction; arrowheads, GFP-Ena spots move rearward. (C) See Movie 2 in the supplementary material. Arrowheads and arrows, large lamellipodial fan with actin microspikes that fuse at distal tips to form filopodia. Scale bars: 5 μm.

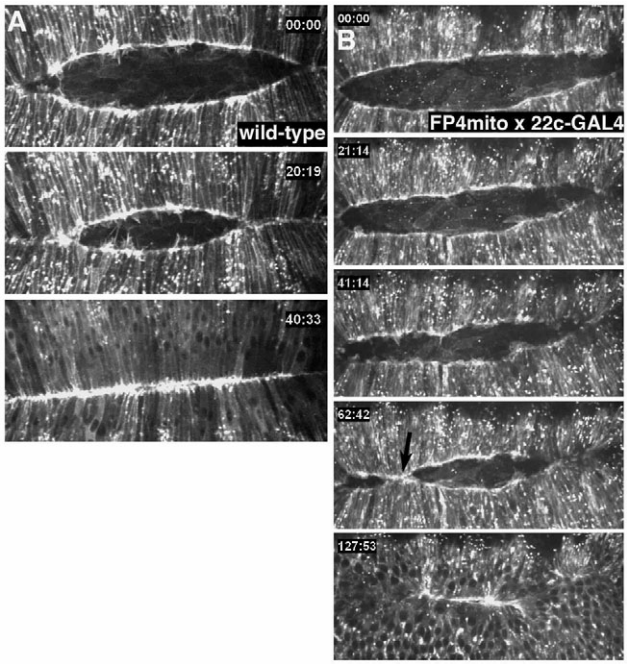

Fig. 8. Ena inactivation slows epithelial zippering. Movie stills showing (**A**) embryos expressing GFP-actin (see Movie 3 in the supplementary material) or (**B**) FP4mito+GFP-actin using e22c-Gal4 (see Movie 4 in the supplementary material). Time, minutes:seconds.

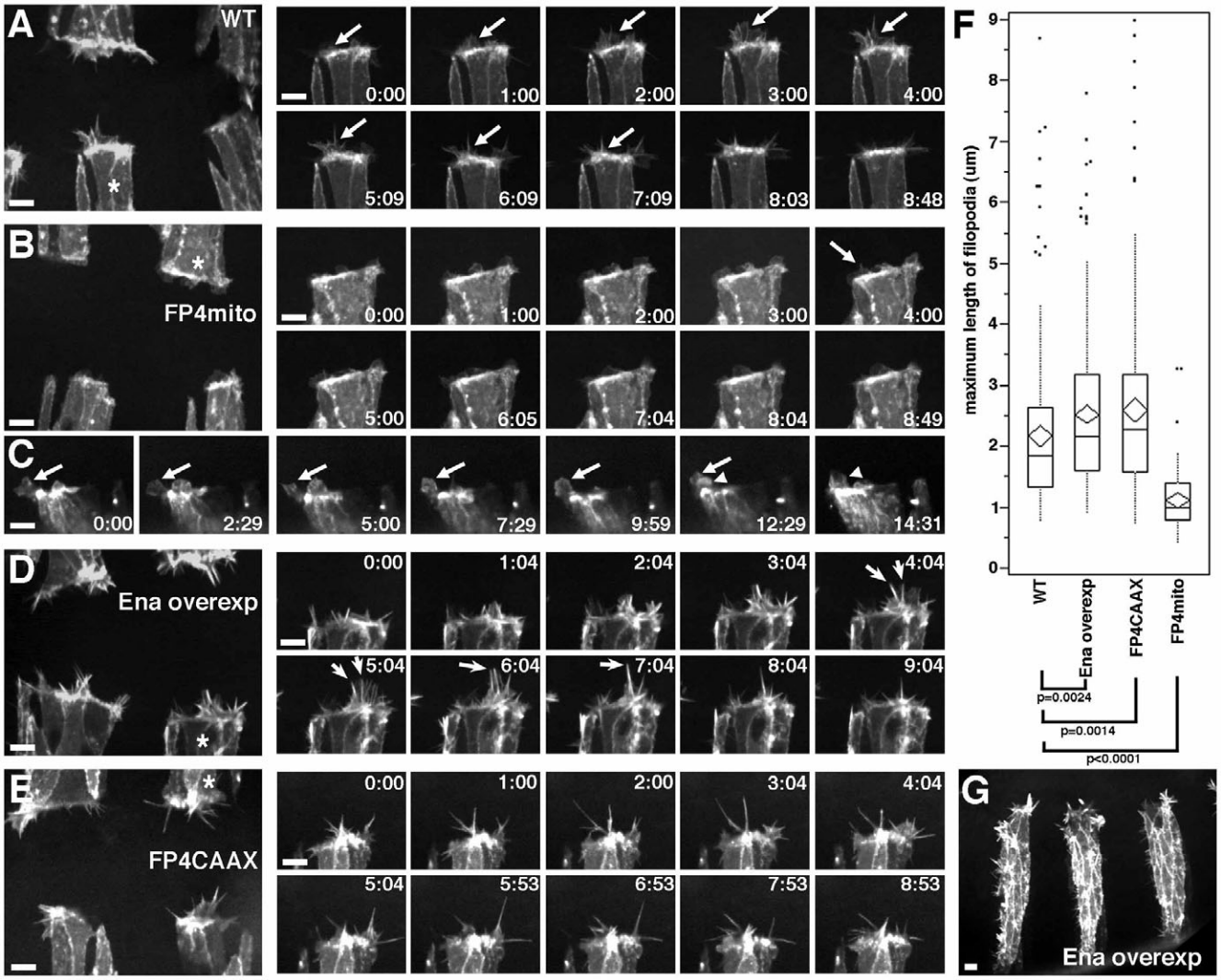

Fig. 9. Altering Ena levels or localization alters membrane protrusions. (**A-E**,**G**) Movie stills showing embryos expressing GFP-actin alone (A) or with FP4mito (B,C), UAS-Ena (Ena overexpression; D,G) or FP4CAAX (E) using *engrailed*-Gal4. Asterisk, *engrailed* stripe in high-magnification series. Time, minutes:seconds. (A) See Movie 5 in the supplementary material. Wild-type. Arrow, lifecycle of lamellipodial-based protrusion. (B) See Movie 5 in the supplementary material. FP4mito. Lamellipodia and rare, short filopodia (arrow, 4:00). (C) FP4mito. Arrow, lamellipodia extended for several minutes; arrowhead, second lamellipodium emerging as first retracts. (D) See Movie 7 in the supplementary material. Ena overexpression. Arrows, fusion of microspikes to form filopodia. (E) FP4CAAX. Longer filopodia. (**F**) Box and whisker plot, maximum filopodial length in leading-edge cells, genotypes indicated. Box, 25th-75th quartile; line across middle, median; diamond, mean±s.d.; broken lines, 10th and 90th percentiles; dots, outliers. *P* values, Student's *t*-test. (G) Ena overexpression induces filopodia on lateral cells. Scale bars: 5 μm.

DISCUSSION

Cell behavior is controlled by regulated cytoskeletal polymerization/depolymerization and by motor proteins interacting with it. Work in cultured cells and in vitro revealed many cytoskeletal regulators and is clarifying their mechanisms of action. A key challenge is to determine how cells utilize this molecular toolkit to drive diverse cell behaviors in a living animal. Ena/VASP proteins are thought to be key parts of this toolkit – work in cell culture suggests important roles in cell migration, actin dynamics and cadherin-based adhesion. However, genetic redundancy in mammals and maternal contribution in flies limited previous analysis of Ena/VASP roles in morphogenesis to *C. elegans*. We inactivated Ena during *Drosophila* embryogenesis, where a dazzling array of cell behaviors allowed us to assess which require Ena.

Assessing the roles of Ena in adhesion and morphogenesis

Drosophila Ena localizes to AJs and regulates cortical actin assembly in follicle cells (Baum and Perrimon, 2001), and Ena/VASP proteins help establish cell adhesion in keratinocytes (Vasioukhin et al., 2000) and mammary epithelial cells (Scott et al., 2006). We first tested the hypothesis that Ena/VASP proteins play key roles in cell-cell adhesion. We were surprised to find that Ena inactivation or mutation did not disrupt AJs or epithelial integrity in embryos or imaginal discs, suggesting that they do not play general roles in these processes. Of course, Ena/VASP proteins may play cell type-specific roles; e.g. filopodial zippers initiating keratinocyte adhesion may require Ena, whereas other mechanisms of establishing epithelial architecture may not. Our data also reveal morphogenetic events in which Ena is nonessential; e.g. there were

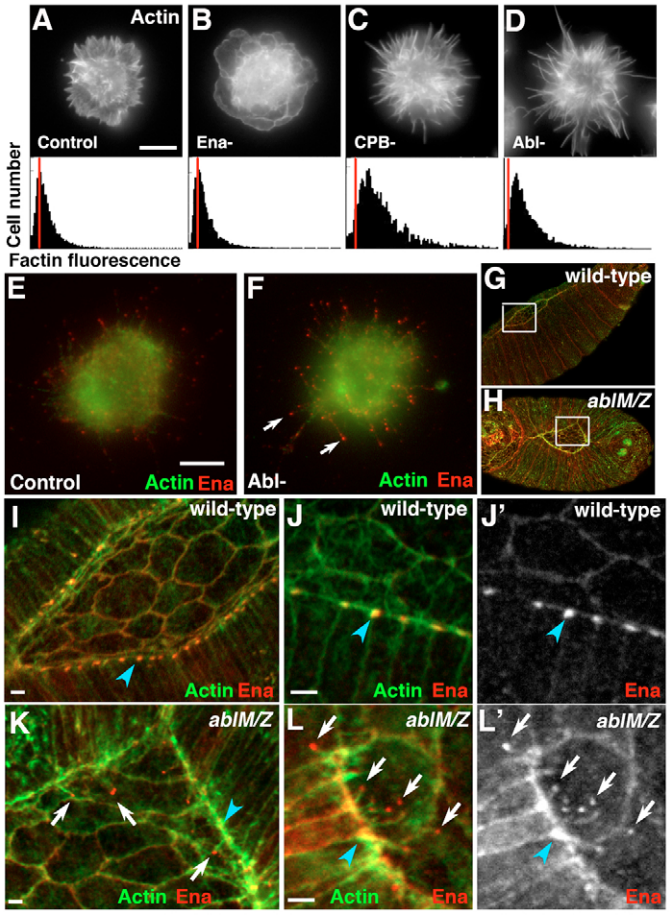

Fig. 10. Filopodial regulation. (**A-D**) Upper panels: F-actin in D16-C3 cells treated for 7 days with indicated dsRNAs; lower panels: histograms showing total F-actin (fluorescent phalloidin) in arbitrary units versus total cell number. Red line, mean actin levels in control cells. (**E-L**) Actin (green); Ena (red). (E,F) Control and *abl* dsRNA. (G-L) M/Z*abl*^{4} and wild type stained in parallel: frames in G and H show areas enlarged in I-L. Scale bars: 5 μm.

no apparent defects in ventral furrows or germband extension. Consistent with this, Mena/VASP/Evl triple mutant mice complete many morphogenetic processes without major defects (F.B.G., unpublished).

Our data did reveal key roles for Ena in many morphogenetic events: germband retraction, head involution, segmental groove retraction and dorsal closure. These build upon previously documented roles for Ena in axon guidance (reviewed by Krause et al., 2003) and actin regulation in follicle cells (Baum and Perrimon, 2001), providing a view of the spectrum of biological events requiring Ena. We hypothesize that Ena acts in a mechanistically similar manner in each process, as an actin anti-Capping protein promoting filament elongation. Flies use this tool in many different ways, promoting distinct cell behaviors.

Some events can be linked fairly directly to known Ena/VASP functions. The role of Ena in axon guidance fits its actin regulatory role well. During dorsal closure, Ena inactivation reduces filopodia, consistent with its biochemical function. Our data reveal that this slows epithelial zippering and disrupts precise alignment between the two sheets. Leading-edge filopodia were proposed to function both as sensors directing proper cell matching, and to facilitate adhesion of cells from opposing edges in *Drosophila* (Jacinto et al., 2000) and *C. elegans* (Williams-Masson et al., 1997). Although our data support a sensory role for filopodia, we did not observe disrupted epithelial adhesion/fusion. Our data support and contrast with work on embryos expressing dominant-negative Cdc42 (Cdc42DN), which produce rudimentary protrusions (Jacinto et al., 2000). Like *ena* mutants, Cdc42DN embryos display mismatching of cells from opposing edges, but, unlike *ena* mutants, Cdc42DN embryos have gaps between cells along the midline. Although Cdc42DN-expressing leading-edge cells produce only rudimentary protrusions, FP4mito-expressing cells produce robust lamellipodia. Because AJ formation in cultured mammalian cells can be mediated either by filopodia (Vasioukhin et al., 2000) or lamellipodia (Ehrlich et al., 2002), lamellipodia may mediate adhesion in the absence of filopodia.

Ena is also essential for morphogenetic events in which its cell biological role is more speculative. Germband retraction requires integrin-mediated adhesion of amnioserosa and epidermis to couple cell-shape changes in the two tissues (Schock and Perrimon, 2002; Schock and Perrimon, 2003). Ena inactivation mimics integrin loss. Ena/VASP proteins localize to focal adhesions, and *Drosophila* Ena colocalizes with integrins at ends of planar-polarized actin bundles in follicle cells (Bateman et al., 2001). Ena/VASP inactivation does not disrupt focal adhesions (Bear et al., 2000), but may modulate their size and stress fiber robustness under mechanical stress (Galler et al., 2005; Yoshigi et al., 2005). *Drosophila* Ena may strengthen the cytoskeleton during germband retraction, promote amnioserosal lamellipodia or regulate extracellular matrix (ECM) adhesion more directly, as VASP does in platelets (reviewed by Krause et al., 2003) and as Ena/VASP proteins may do in *Xenopus* somitogenesis (Kragtorp and Miller, 2006). Less is known about mechanisms by which segmental grooves form and retract (Larsen et al., 2003). However, Ena is planar-polarized to dorsal-ventral cell boundaries in these cells; perhaps it stabilizes actin attachment at borders where it is enriched. Defects in head involution result from alterations in dorsal-fold cell shape change, which may share mechanistic similarities with segmental groove formation.

Ena and filopodia in vivo

One key challenge is to identify machinery required to generate filopodia and lamellipodia. We found a striking correlation between Ena activity and filopodial length and number. Inactivating Ena significantly decreased filopodial length and number, whereas increasing Ena activity increased filopodial length. Interestingly, maximum filopodial length was not substantially altered, and thus is probably not limited by Ena levels. However, Ena can be rate-limiting in filopodial formation as Ena overexpression generated filopodia on lateral epithelial cells that normally do not produce them. Together, these data suggest that Ena promotes both initiation and elongation of leading-edge filopodia.

Ena is concentrated at the tips of elongating filopodia, consistent with its influence on filopodial length and its biochemical function. Interestingly, GFP-Ena particles move rearward prior to retraction, presumably by retrograde flow, and some GFP-Ena is retained at filopodial tips as they retract. We had not expected this, as the anti-capping function of Ena/VASP suggested that Ena at filopodial tips would promote extension. Although this could be an artifact of GFP-Ena, it may indicate complexity in the control of filopodial dynamics. For example, whether filopodia continue extending or retract may be determined not only by actin polymerization rates at the tip, but also by depolymerization and/or retrograde flow rates at its base. In addition, filopodial dynamics may be regulated at

individual filaments within filopodia rather than the structure as a whole. GFP-Ena particles may be locally inactivated Ena on individual filaments moving away from the tip by retrograde flow.

One unanswered question is whether different filopodial regulators act additively or in series. Mammalian Ena/VASP can act downstream of Cdc42 together with IRSp53 (Krugmann et al., 2001), but IRSp53 can promote Ena/VASP-independent filopodia (Nakagawa et al., 2003). Formins also promote filopodia, but whereas *Dictyostelium* dDia2 and VASP directly interact, Ena/VASP:formin relationships remain unclear (reviewed by Faix and Rottner, 2006). The reduced number of short filopodia formed when Ena is inactivated is consistent with multiple mechanisms acting additively/synergistically to produce the appropriate filopodial number/length.

Our data also test in vivo one aspect of the convergent elongation model (Svitkina et al., 2003). This proposes that tip complex proteins bind filaments and protect them from capping, allowing continued elongation, and then interact laterally, bundling filaments and forming filopodia. Ena/VASP proteins may supply anti-capping activity, and could also help mediate lateral association via tetramerization. GFP-Ena overexpression promoted large lamellipodia containing numerous actin microspikes; these often converged at their distal ends to form filopodia, supporting the convergent elongation model.

We also examined filopodial regulation. Our data demonstrate that Abl is a key negative regulator of filopodial extension in cultured cells and in vivo, inhibiting Ena accumulation at nascent filopodial tips. This idea is further supported by our parallel analysis of embryos expressing activated Bcr-Abl or excess wild-type Abl; both reduce filopodia on leading-edge and amnioserosal cells (T. Stevens and M.P., unpublished). This provides a means for signal transduction pathways to regulate cell behavior.

We thank P. Martin, the Bloomington *Drosophila* Stock Center and the Developmental Studies Hybridoma Bank for reagents, and T. Harris, D. Fox and R. Cheney for helpful comments. This work was supported by NIHGM47857 to M.P. J.G. is a Leukemia and Lymphoma Society Special Fellow. J.G. was supported by NIH5F32GM068337, J.P.M. by the Smallwood Foundation and a Goldwater Scholarship, M.E. by an HHMI Predoctoral Fellowship, D.V.V. by a Leukemia and Lymphoma Scholarship and grants from the National Institute of Neurological Disorders and Stroke, and F.B.G. by NIHGM58801.

Supplementary material

Supplementary material for this article is available at http://dev.biologists.org/cgi/content/full/134/11/2027/DC1

References

Ahern-Djamali, S. M., Comer, A. R., Bachmann, C., Kastenmeier, A. S., Reddy, S. K., Beckerle, M. C., Walter, U. and Hoffmann, F. M. (1998). Mutations in Drosophila enabled and rescue by human vasodilator-stimulated phosphoprotein (VASP) indicate important functional roles for Ena/VASP homology domain 1 (EVH1) and EVH2 domains. *Mol. Biol. Cell* **9**, 2157-2171.

Ball, L. J., Jarchau, T., Oschkinat, H. and Walter, U. (2002). EVH1 domains: structure, function and interactions. *FEBS Lett.* **513**, 45-52.

Barzik, M., Carl, U. D., Schubert, W. D., Frank, R., Wehland, J. and Heinz, D. W. (2001). The N-terminal domain of Homer/Vesl is a new class II EVH1 domain. *J. Mol. Biol.* **309**, 155-169.

Barzik, M., Kotova, T. I., Higgs, H. N., Hazelwood, L., Hanein, D., Gertler, F. B. and Schafer, D. A. (2005). Ena/VASP proteins enhance actin polymerization in the presence of barbed end capping proteins. *J. Biol. Chem.* **280**, 28653-28662.

Bashaw, G. J., Kidd, T., Murray, D., Pawson, T. and Goodman, C. S. (2000). Repulsive axon guidance: Abelson and Enabled play opposing roles downstream of the roundabout receptor. *Cell* **101**, 703-715.

Bateman, J., Reddy, R. S., Saito, H. and Van Vactor, D. (2001). The receptor tyrosine phosphatase Dlar and integrins organize actin filaments in the Drosophila follicular epithelium. *Curr. Biol.* **11**, 1317-1327.

Baum, B. and Perrimon, N. (2001). Spatial control of the actin cytoskeleton in Drosophila epithelial cells. *Nat. Cell Biol.* **3**, 883-890.

Bear, J. E., Loureiro, J. J., Libova, I., Fassler, R., Wehland, J. and Gertler, F. B. (2000). Negative regulation of fibroblast motility by Ena/VASP proteins. *Cell* **101**, 717-728.

Bear, J. E., Svitkina, T. M., Krause, M., Schafer, D. A., Loureiro, J. J., Strasser, G. A., Maly, I. V., Chaga, O. Y., Cooper, J. A., Borisy, G. G. et al. (2002). Antagonism between Ena/VASP proteins and actin filament capping regulates fibroblast motility. *Cell* **109**, 509-521.

Beneken, J., Tu, J. C., Xiao, B., Nuriya, M., Yuan, J. P., Worley, P. F. and Leahy, D. J. (2000). Structure of the Homer EVH1 domain-peptide complex reveals a new twist in polyproline recognition. *Neuron* **26**, 143-154.

Brand, A. H. and Perrimon, N. (1993). Targeted gene expression as a means of altering cell fates and generating dominant phenotypes. *Development* **118**, 401-415.

Chang, C., Adler, C. E., Krause, M., Clark, S. G., Gertler, F. B., Tessier-Lavigne, M. and Bargmann, C. I. (2006). MIG-10/lamellipodin and AGE-1/PI3K promote axon guidance and outgrowth in response to slit and netrin. *Curr. Biol.* **16**, 854-862.

Cox, R. T., Kirkpatrick, C. and Peifer, M. (1996). Armadillo is required for adherens junction assembly, cell polarity, and morphogenesis during *Drosophila* embryogenesis. *J. Cell Biol.* **134**, 133-148.

Dent, E. W. and Gertler, F. B. (2003). Cytoskeletal dynamics and transport in growth cone motility and axon guidance. *Neuron* **40**, 209-227.

Ehrlich, J. S., Hansen, M. D. and Nelson, W. J. (2002). Spatio-temporal regulation of Rac1 localization and lamellipodia dynamics during epithelial cell-cell adhesion. *Dev. Cell* **3**, 259-270.

Faix, J. and Rottner, K. (2006). The making of filopodia. *Curr. Opin. Cell Biol.* **18**, 18-25.

Galler, A. B., Garcia Arguinzonis, M. I., Baumgartner, W., Kuhn, M., Smolenski, A., Simm, A. and Reinhard, M. (2005). VASP-dependent regulation of actin cytoskeleton rigidity, cell adhesion, and detachment. *Histochem. Cell Biol.* **115**, 457-474.

Gertler, F. B., Comer, A. R., Juang, J., Ahern, S. M., Clark, M. J., Liebl, E. C. and Hoffmann, F. M. (1995). *enabled*, a dosage-sensitive suppressor of mutations in the *Drosophila* Abl tyrosine kinase, encodes an Abl substrate with SH3 domain-binding properties. *Genes Dev.* **9**, 521-533.

Gitai, Z., Yu, T. W., Lundquist, E. A., Tessier-Lavigne, M. and Bargmann, C. I.. (2003). The netrin receptor UNC-40/DCC stimulates axon attraction and outgrowth through enabled and, in parallel, Rac and UNC-115/AbLIM. *Neuron* **37**, 53-65.

Grevengoed, E. E., Loureiro, J. J., Jesse, T. L. and Peifer, M. (2001). Abelson kinase regulates epithelial morphogenesis in Drosophila. *J. Cell Biol.* **155**, 1185-1198.

Grevengoed, E. E., Fox, D. T., Gates, J. and Peifer, M. (2003). Balancing different types of actin polymerization at distinct sites: roles for Abelson kinase and Enabled. *J. Cell Biol.* **163**, 1267-1279.

Han, Y. H., Chung, C. Y., Wessels, D., Stephens, S., Titus, M. A., Soll, D. R. and Firtel, R. A. (2002). Requirement of a vasodilator-stimulated phosphoprotein family member for cell adhesion, the formation of filopodia, and chemotaxis in dictyostelium. *J. Biol. Chem.* **277**, 49877-49887.

Hutson, M. S., Tokutake, Y., Chang, M. S., Bloor, J. W., Venakides, S., Kiehart, D. P. and Edwards, G. S. (2003). Forces for morphogenesis investigated with laser microsurgery and quantitative modeling. *Science* **300**, 145-149.

Jacinto, A., Wood, W., Balayo, T., Turmaine, M., Martinez-Arias, A. and Martin, P. (2000). Dynamic actin-based epithelial adhesion and cell matching during Drosophila dorsal closure. *Curr. Biol.* **10**, 1420-1426.

Kiehart, D. P., Galbraith, C. G., Edwards, K. A., Rickoll, W. L. and Montague, R. A. (2000). Multiple forces contribute to cell sheet morphogenesis for dorsal closure in Drosophila. *J. Cell Biol.* **149**, 471-490.

Kragtorp, K. A. and Miller, J. R. (2006). Regulation of somitogenesis by Ena/VASP proteins and FAK during Xenopus development. *Development* **133**, 685-695.

Krause, M., Dent, E. W., Bear, J. E., Loureiro, J. J. and Gertler, F. B. (2003). Ena/VASP proteins: regulators of the actin cytoskeleton and cell migration. *Annu. Rev. Cell Dev. Biol.* **19**, 541-564.

Krugmann, S., Jordens, I., Gevaert, K., Driessens, M., Vandekerckhove, J. and Hall, A. (2001). Cdc42 induces filopodia by promoting the formation of an IRSp53:Mena complex. *Curr. Biol.* **11**, 1645-1655.

Lanier, L. M., Gates, M. A., Witke, W., Menzies, A. S., Wehman, A. M., Macklis, J. D., Kwiatkowski, D., Soriano, P. and Gertler, F. B. (1999). Mena is required for neurulation and commissure formation. *Neuron* **22**, 313-325.

Larsen, C. W., Hirst, E., Alexandre, C. and Vincent, J. P. (2003). Segment boundary formation in Drosophila embryos. *Development* **130**, 5625-5635.

Lebrand, C., Dent, E. W., Strasser, G. A., Lanier, L. M., Krause, M., Svitkina, T. M., Borisy, G. G. and Gertler, F. B. (2004). Critical role of Ena/VASP proteins for filopodia formation in neurons and in function downstream of netrin-1. *Neuron* **42**, 37-49.

Mejillano, M. R., Kojima, S., Applewhite, D. A., Gertler, F. B., Svitkina,T. M. and Borisy, G. G. (2004). Lamellipodial versus filopodial mode of the actin nanomachinery: pivotal role of the filament barbed end. *Cell* **118**, 363-373.

Menzies, A. S., Aszodi, A., Williams, S. E., Pfeifer, A., Wehman, A. M., Goh, K. L., Mason, C. A., Fassler, R. and Gertler, F. B. (2004). Mena and vasodilator-stimulated phosphoprotein are required for multiple actin-dependent processes that shape the vertebrate nervous system. *J. Neurosci.* **24**, 8029-8038.
Nakagawa, H., Miki, H., Nozumi, M., Takenawa, T., Miyamoto, S., Wehland, J. and Small, J. V. (2003). IRSp53 is colocalised with WAVE2 at the tips of protruding lamellipodia and filopodia independently of Mena. *J. Cell Sci.* **116**, 2577-2583.
Pollard, T. D. and Borisy, G. G. (2003). Cellular motility driven by assembly and disassembly of actin filaments. *Cell* **112**, 453-465.
Rogers, S. L., Rogers, G. C., Sharp, D. J. and Vale, R. D. (2002). Drosophila EB1 is important for proper assembly, dynamics, and positioning of the mitotic spindle. *J. Cell Biol.* **158**, 873-884.
Rogers, S. L., Wiedemann, U., Stuurman, N. and Vale, R. D. (2003). Molecular requirements for actin-based lamella formation in Drosophila S2 cells. *J. Cell Biol.* **162**, 1079-1088.
Rogers, S. L., Wiedemann, U., Hacker, U., Turck, C. and Vale, R. D. (2004). Drosophila RhoGEF2 associates with microtubule plus ends in an EB1-dependent manner. *Curr. Biol.* **14**, 1827-1833.
Samarin, S., Romero, S., Kocks, C., Didry, D., Pantaloni, D. and Carlier, M. F. (2003). How VASP enhances actin-based motility. *J. Cell Biol.* **163**, 131-142.
Schock, F. and Perrimon, N. (2002). Cellular processes associated with germ band retraction in Drosophila. *Dev. Biol.* **248**, 29-39.
Schock, F. and Perrimon, N. (2003). Retraction of the Drosophila germ band requires cell-matrix interaction. *Genes Dev.* **17**, 597-602.
Scott, J. A., Shewan, A. M., den Elzen, N. R., Loureiro, J. J., Gertler, F. B. and Yap, A. S. (2006). Ena/VASP proteins can regulate distinct modes of actin organization at cadherin-adhesive contacts. *Mol. Biol. Cell* **17**, 1085-1095.
Shakir, M. A., Gill, J. S. and Lundquist, E. A. (2006). Interactions of UNC-34 Enabled with Rac GTPases and the NIK kinase MIG-15 in C. elegans axon pathfinding and neuronal migration. *Genetics* **172**, 893-913.
Svitkina, T. M., Bulanova, E. A., Chaga, O. Y., Vignjevic, D. M., Kojima, S., Vasiliev, J. M. and Borisy, G. G. (2003). Mechanism of filopodia initiation by reorganization of a dendritic network. *J. Cell Biol.* **160**, 409-421.
Vasioukhin, V., Bauer, C., Yin, M. and Fuchs, E. (2000). Directed actin polymerization is the driving force for epithelial cell-cell adhesion. *Cell* **100**, 209-219.
Volkman, B. F., Prehoda, K. E., Scott, J. A., Peterson, F. C. and Lim, W. A. (2002). Structure of the N-WASP EVH1 domain-WIP complex: insight into the molecular basis of Wiskott-Aldrich Syndrome. *Cell* **111**, 565-576.
Wieschaus, E. and Nüsslein-Volhard, C. (1986). Looking at embryos. In *Drosophila, A Practical Approach* (ed. D. B. Roberts), pp. 199-228. Oxford: IRL Press.
Williams-Masson, E. M., Malik, A. N. and Hardin, J. (1997). An actin-mediated two-step mechanism is required for ventral enclosure of the C. elegans hypodermis. *Development* **124**, 2889-2901.
Wills, Z., Bateman, J., Korey, C. A., Comer, A. and Van Vactor, D. (1999). The tyrosine kinase Abl and its substrate enabled collaborate with the receptor phosphatase Dlar to control motor axon guidance. *Neuron* **22**, 301-312.
Withee, J., Galligan, B., Hawkins, N. and Garriga, G. (2004). Caenorhabditis elegans WASP and Ena/VASP proteins play compensatory roles in morphogenesis and neuronal cell migration. *Genetics* **167**, 1165-1176.
Yoshigi, M., Hoffman, L. M., Jensen, C. C., Yost, H. J. and Beckerle, M. C. (2005). Mechanical force mobilizes zyxin from focal adhesions to actin filaments and regulates cytoskeletal reinforcement. *J. Cell Biol.* **171**, 209-215.
Yu, T. W., Hao, J. C., Lim, W., Tessier-Lavigne, M. and Bargmann, C. I. (2002). Shared receptors in axon guidance: SAX-3/Robo signals via UNC-34/Enabled and a Netrin-independent UNC-40/DCC function. *Nat. Neurosci.* **5**, 1147-1154.
Zettl, M. and Way, M. (2002). The WH1 and EVH1 domains of WASP and Ena/VASP family members bind distinct sequence motifs. *Curr. Biol.* **12**, 1617-1622.